Evaluation of AISC Seismic Design Methods for Steel Multi-Tiered Special Concentrically Braced Frames

PABLO A. CANO and ALI IMANPOUR

ABSTRACT

Steel multi-tiered concentrically braced frames (MT-CBFs) are commonly used in North America as a lateral load resisting system of tall single-story buildings. Past studies show that MT-CBF columns designed in accordance with the 2010 AISC *Seismic Provisions* are prone to buckling due to a high axial compression force combined with in-plane bending moments caused by the nonuniform distribution of inelastic brace deformations along the frame height. Special design provisions have been introduced in the 2016 AISC *Seismic Provisions* to address flexural demands imposed on MT-CBF columns and prevent column instability. In this paper, the seismic design methods for multi-tiered special concentrically braced frames are evaluated using the nonlinear finite element analysis method. A two-tiered special concentrically braced frame was then created, and nonlinear static and dynamic analyses were performed to evaluate the seismic performance of both frames. Analysis results confirmed that the inelastic deformations in the frame designed using the 2010 requirements are not uniformly distributed but rather concentrated in one of the tiers and cause column instability under large story drifts, whereas, the 2016 design method significantly improves the distribution of inelastic deformation along the height of the frame and prevents column instability. Furthermore, it was found that the 2016 AISC *Seismic Provisions* accurately estimate the axial load but overestimate the in-plane flexural demands and underestimates the out-of-plane flexural demand. Nonetheless, the overestimation of in-plane flexure demands results in acceptable strength capacity even though out-of-plane flexural demands is underestimated.

Keywords: Steel multi-tiered concentrically braced frame, design standards, column buckling, cyclic-pushover analysis.

INTRODUCTION

Steel multi-tiered concentrically braced frames (MT-CBFs) are widely used in North America as a lateral-resisting system of tall, single-story buildings such as airplane hangars, recreational facilities, shopping centers and industrial buildings. MT-CBFs consist of multiple bracing panels stacked along the height of the building and are separated by horizontal struts as illustrated in Figure 1(a). Intermediate struts are used between braced panels to avoid unsatisfactory K-braced frame (K-BF) response. Various bracing configurations—including chevron, diagonal, V-type, and cross—are used in MT-CBFs. Two examples of such frames with cross bracing configuration is shown in Figures 1(b) and 1(c). Multi-tiered arrangements are typically used when it is not practical or economical to use a single bracing panel along the height of the frame. In MT-CBFs, the length of the braces is reduced, resulting in a lower slenderness ratio, which allows for smaller brace sizes to resist lateral loads and a more efficient angle between the brace and the horizontal plane of the frame. Additionally, the buckling length of the column in the plane of the frame is reduced as the intermediate struts provide lateral support for in-plane buckling. This framing configuration is also beneficial when frames are designed to resist seismic load effects. The limits on width-to-thickness and global slenderness ratios can be easily satisfied when using shorter braces. Moreover, reduced brace sizes result in smaller design forces on the adjacent members, including struts, beams, columns, connections, and footing.

MT-CBF columns are typically W-shaped members oriented such that out-of-plane bending moment due to the wind load acts about the major axis of the section. The columns can be considered braced in the plane of the frame as a result of horizontal struts; however, no out-of-plane bracing exists between the ground and roof levels, and the column buckling length is equal to the full-frame height in this direction.

Two concentrically braced frame systems have been defined in the AISC *Seismic Provisions* (AISC, 2010, 2016a): ordinary concentrically braced frames (OCBFs) and special concentrically braced frames (SCBFs). Braces of both OCBFs and SCBFs are sized to resist the seismic load effects under the design seismic base shear. In SCBFs, the columns are designed under the axial loads due to the combined gravity loads and the axial capacity of the braces when they respond in the inelastic range. The columns of OCBFs are, however, designed to resist the overstrength seismic load. The 2010 AISC *Seismic Provisions* (AISC, 2010) did not include design provisions for MT-CBFs. The

Pablo A. Cano, E.I.T, M.Sc., Ph.D. Student, University of Alberta, Edmonton, Alberta. Email: cano@ualberta.ca (corresponding)

Ali Imanpour, P.Eng., Ph.D., Assistant Professor, University of Alberta, Edmonton, Alberta. Email: imanpour@ualberta.ca

Paper No. 2019-17

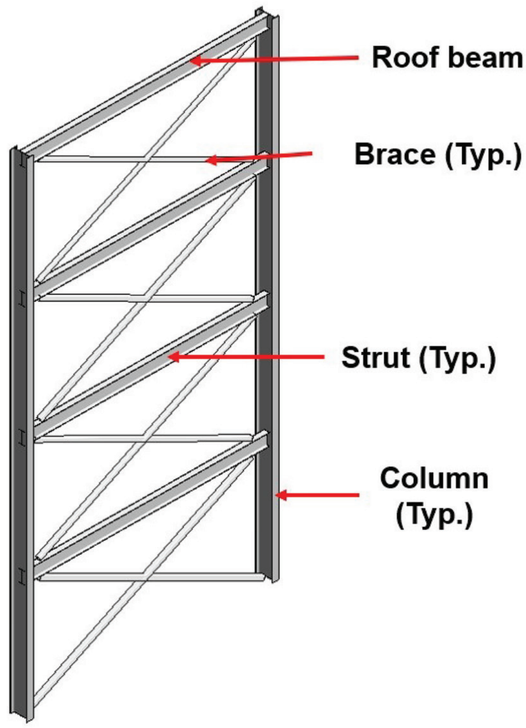

(a) Multi-tiered concentrically braced frame components

(b) Two-tiered concentrically braced frame

(c) Four-tiered concentrically braced frame

Fig. 1. Multi-tiered concentrically braced frames.

two brace loading analysis cases for SCBFs in this standard led engineers to recognize the potential for unbalanced loads at the intermediate tier due to the violation of the equilibrium when such brace loading scenarios are considered. As such, this framing configuration over time came to be considered a K-brace, a framing system that is prohibited by the AISC *Seismic Provisions*. In the absence of special design provisions, MT-CBFs had been designed using the provisions prescribed for multi-story steel braced frames in Section F of the 2010 AISC *Seismic Provisions*.

The seismic behavior of MT-CBFs designed using the 2010 *Seismic Provisions* has been the focus of a number of research studies in recent years (Imanpour and Tremblay, 2012, 2014; Imanpour et al., 2013, 2016a). The results obtained from past numerical simulations confimed that inelastic frame deformations tend to concentrate in a single tier rather than be uniformly distributed along the height of the frame. The reason is that tensile yielding is only initiated in the tier that has the lowest story shear resistance; this tier is referred to as the critical tier. Even if tiers are identical, slight variations between the brace properties such as material properties, initial geometric imperfections, or end conditions can lead to the initiation of brace yielding in one of the tiers. This response is illustrated in Figure 2(a) for the two-tiered CBF. As shown in Figure 2(b), the compression braces buckle nearly simultaneously in both tiers. As the lateral displacement at the roof level increases, tensile yielding initiates only in one of the tiers [i.e., Tier 1 as shown in Figure 2(c)], which reduces the story shear resistance of that tier and attracts the rest of the lateral deformations, thus preventing tensile yielding of the tension brace in the adjacent tiers. By further elongation of the tensile brace after yielding, excessive inelastic deformations are induced in the critical tier. The difference between the story

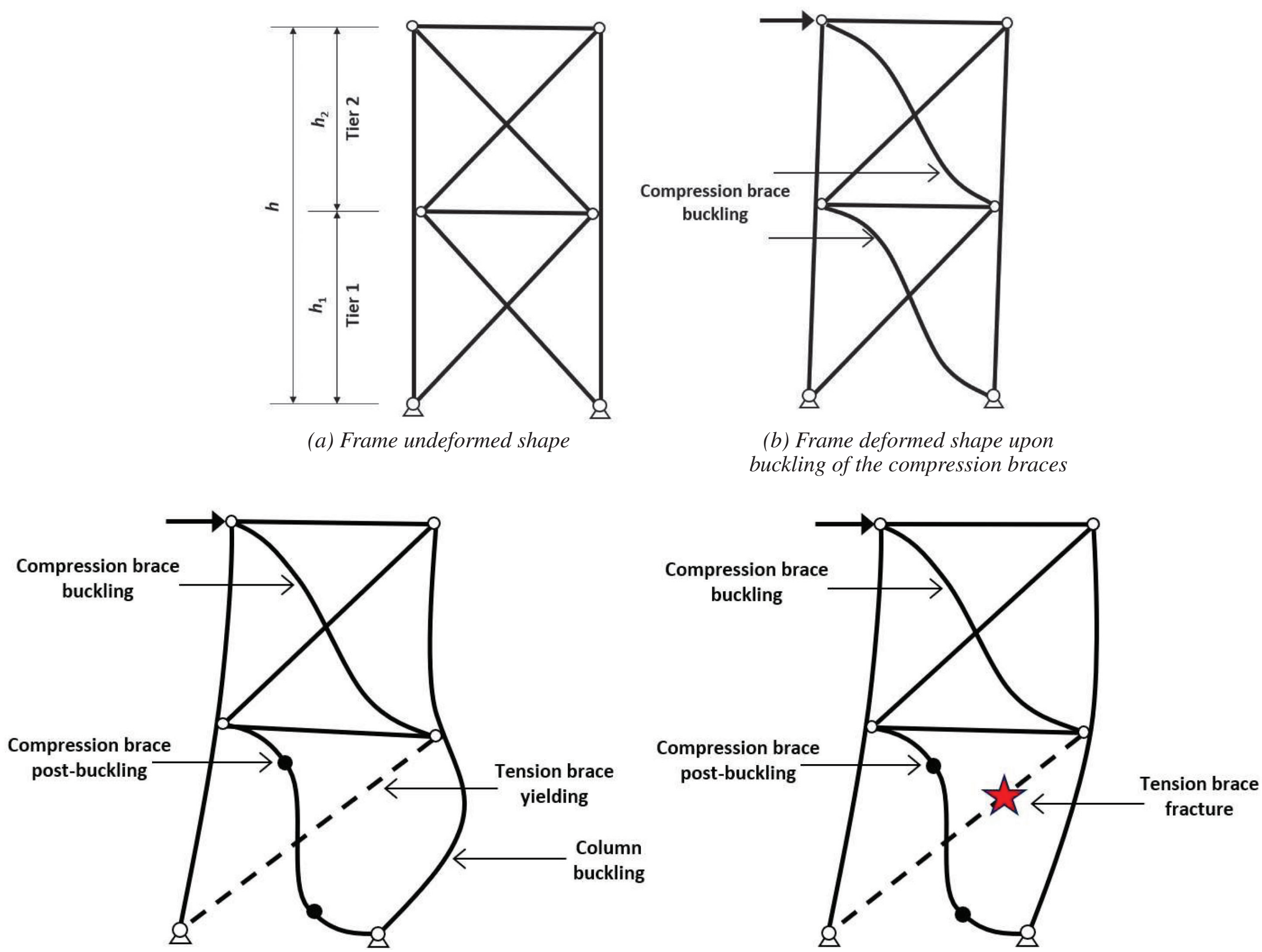

(a) Frame undeformed shape

(b) Frame deformed shape upon buckling of the compression braces

(c) Column buckling

(d) Tension brace fracture

Fig. 2. Inelastic response of MT-CBFs.

shear resistance of the adjacent tiers induces an unbalanced horizontal shear force on the columns of the frame, which results in large in-plane bending moments in the columns. The concentration of inelastic deformations in the critical tier can lead to column yielding under the combination of high axial compression force and bending moments if the columns do not possess sufficient strength and stiffness. Such large demands may lead to column buckling as shown in Figure 2(c) and even frame collapse. It was found that column instability is first initiated in the plane of the frame in a flexural buckling mode and suddenly changes to a flexural-torsional buckling mode as excessive out-of-plane displacements develop at the frame mid-height. In addition to column instability, excessive brace deformations that take place only in one of the tiers can lead to low cyclic fatigue fracture of the brace (Tremblay et al., 2003; Hsiao et al., 2013) as shown in Figure 2(d).

Stoakes and Fahnestock (2014, 2016) showed that providing torsional bracing, along the height of the column at the strut-to-column connections, can improve the strong-axis buckling strength in the presence of in-plane flexural yielding, particularly when the location of the weak-axis flexural moment matches the location of the strong-axis flexural moment. More recently, Imanpour et al. (2018) examined the seismic performance of an MT-CBF designed in accordance with the 2010 AISC *Seismic Provisions* using hybrid simulation where the first-tier column segment was tested experimentally, while the rest of the frame was analyzed numerically. The results of hybrid simulations confirmed the column instability observed in previous numerical simulations. A preliminary study was recently performed by the authors to evaluate the seismic response of multi-tiered concentrically braced frames designed in accordance with the 2010 and 2016 *Seismic Provisions* (AISC, 2010, 2016a; Cano and Imanpour, 2018, 2019). The results provide insight into the behavior of MT-CBFs designed in accordance with the 2016 *Seismic Provisions* and also the unfavorable failure modes of frames designed in accordance with the 2010 *Seismic Provisions* frames such as column buckling and frame collapse.

The 2016 AISC *Seismic Provisions* have introduced special design requirements for both multi-tiered OCBFs and SCBFs to address the unsatisfactory response of MT-CBFs observed in previous studies. Although significant improvements have been made over the past decade in the seismic design methodologies of multi-tiered braced frames, it is felt that there is limited information to validate and improve the recently adopted design requirements. In particular, the in-plane and out-of-plane bending moment demands prescribed by the current AISC *Seismic Provisions* must be examined and improved if necessary.

This paper aims to examine and compare the seismic design methods for steel multi-tiered special concentrically braced frames (MT-SCBFs) designed in accordance with the 2010 and 2016 AISC *Seismic Provisions*. In particular the paper serves to confirm the improved seismic performance expected when the 2016 provisions are employed. A review of the current and previous seismic design provisions is first given. The seismic design of a case study two-tiered SCBF in accordance with both provisions is then presented followed by the analysis of the seismic response of the frames using nonlinear static (pushover) and nonlinear dynamic (response history) analyses. Finally, the analysis results including the drifts and column moment demands are discussed and used to evaluate the column design demands.

AISC *SEISMIC PROVISIONS* FOR THE DESIGN OF STEEL MT-SCBFS

2010 AISC *Seismic Provisions*

In the 2010 AISC *Seismic Provisions*, no special design guidelines existed for the design of MT-SCBFs. In lieu of such provisions, the requirements for standard SCBFs were used in design. Two analysis cases (A and B) were considered in Section F2.3 representing the brace nonlinear response to determine the forces in the members adjacent to the bracing members, such as columns, struts, beams, and their connections. Analysis cases A and B are shown in Figures 3(a) and 3(b) for a two-tiered braced frame, respectively. In analysis case A, the tension braces reach their expected tensile strength, T_{exp}, and compression braces reach their expected buckling strength, C_{exp}. Moreover, the second analysis case represents the frame response after experiencing several inelastic cycles where the tension braces elongated in tension, but their strength can still be estimated by the expected tensile strength, T_{exp}, while the compression braces reach their expected post-buckling strength, C'_{exp}. These two analysis cases result in seismic axial forces in the columns and struts of MT-SCBFs, which are used to size these members. The effect of gravity loads must be also considered for the design of columns and the roof beam.

2016 AISC *Seismic Provisions*

Past numerical simulations showed that the seismic-induced demands in multi-tiered braced frames differ from those in standard multi-story concentrically braced frames, which, if not considered in the design, may result in column instability or excessive brace elongation that can lead to brace fracture (Imanpour and Tremblay, 2014; Imanpour et al., 2016a). The 2016 AISC *Seismic Provisions* have introduced design requirements for ordinary and special concentrically braced frames as well as buckling-restraint braced frames to prevent such unsatisfactory limit states in the braced frames with multi-tiered configurations. According to the 2016 AISC *Seismic Provisions* Section F2.3(c), MT-SCBFs must be analyzed under the new analysis case (C) in addition to analysis cases A and B applied to all other SCBFs. This new analysis case is shown in Figure 3(c) for a two-tiered braced frame. Analysis case C represents the progressive yielding and buckling of braces in MT-SCBFs, meaning that brace tensile yielding has occurred in the tier that possesses the least story shear resistance (critical tier) [i.e., Tier 1 in Figure 3(c)] and propagates to the strongest tier [Tier 2 in Figure 3(c)]. In analysis case C, it is assumed that the compression brace in the critical tier has reached its post-buckling strength, C'_{exp}, and the compression brace in the noncritical tier has reached its expected buckling strength, C_{exp}. Concurrently, the tension brace in both tiers is assumed to be at their expected tension strength, T_{exp}.

In the case of frames with more than three tiers, the compression forces can be taken equal to their expected buckling strength while the tension forces are below their expected tension strength, which can be computed using an equilibrium knowing that tiers have an identical story shear. For a two-tiered braced frame similar to the one shown in Figure 2(a), analysis case C requires only one step when the critical tier is known; however, analysis case C must be repeated with the critical tier being Tier 2 if the difference between the story shear resistances is negligible to account for potential variabilities in the brace material (Schmidt and Barlett, 2002), brace length connection details, or initial geometric imperfections. The designer can set the criterion to identify the critical tier based on the story shear resistance (e.g., a difference between the story shear resistances less than 10% would be deemed sufficient to examine other plausible critical cases). This would mean that multiple analyses are needed when designing frames with three or more bracing tiers under analysis case C. As a result of this analysis case, columns are subjected not only to an axial force, but also to an in-plane bending moment due to the difference between the shear forces in the braces of adjacent tiers, which creates an unbalanced brace story shear force on the columns. To obtain the column bending moments in a two-tiered braced frame, half of the unbalanced brace story shear force, which is determined under the brace expected forces, is used on a simply supported column spanning between the tiers. This method can be expanded to frames with three or more tiers when brace tension yielding propagates progressively starting from the bottom tier or from the top one (Imanpour and Tremblay, 2016; Imanpour et al., 2016b).

In addition to the new analysis case that results in column in-plane moment demands, an out-of-plane bending moment demand must be considered in design of columns as outlined in AISC *Seismic Provisions* Section F2.4e(c)(3). Out-of-plane bending moments are induced in the columns of multi-tiered braced frames as a result of initial geometric imperfections, out-of-plane buckling of braces, and plastic hinge forming in the brace gusset plate. The 2016 AISC *Seismic Provisions* require a horizontal notional load be applied on the column at the tier level to produce an out-of-plane bending moment demand on the column, representing imperfection effects. The notional load is equal to 0.006 times the vertical component of the compression brace that meets the column at the tier level. This notional load should be amplified by the B_1 factor (AISC, 2016b) to account for P-δ effects. Furthermore, the columns must be designed to resist the out-of-plane moment produced by the buckling

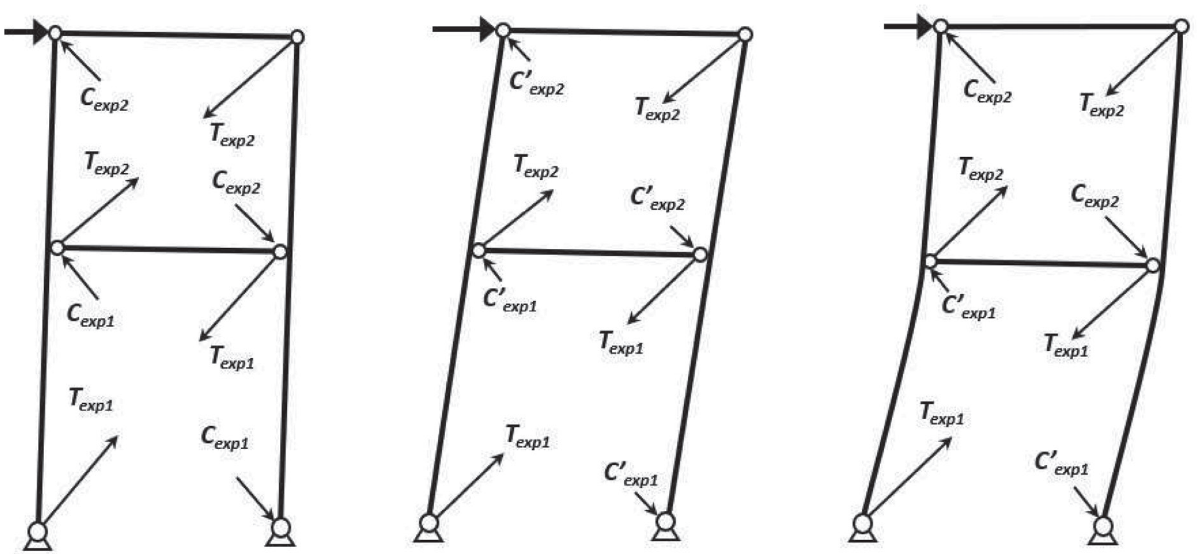

(a) Analysis case A *(b) Analysis case B* *(c) Analysis case C*

Fig. 3. Brace loading scenarios used for the design of capacity-controlled members.

of the braces, but less than the maximum bending moment resistance of the brace connections.

As required in the 2016 AISC *Seismic Provisions* Section F2.4e(b)(1), MT-CBFs must also have intermediate struts placed between adjacent tiers to prevent the unsatisfactory K-braced frame response. Furthermore, columns must be torsionally braced at the strut-to-column connections as per Section F2.4e(c)(1). Finally, AISC *Seismic Provisions* Section F2.4e(d) has established a maximum tier drift ratio of 2% to prevent excessive brace deformations that can cause brace low-cycle fatigue fracture.

BUILDING CONFIGURATION AND LOADING FOR CASE STUDY

Building Geometry

A single-story steel building located in Seattle, Washington, was selected as a case study. The building has plan dimensions of 115 ft × 620 ft with a height of h = 29.5 ft. In each principal direction, the building has four concentrically braced frames (two per each exterior wall). The frame height is divided into two tiers with X-bracing configuration as shown in Figure 4. As illustrated, the bottom tier (Tier 1) height is h_1 = 15.4 ft, and the top tier (Tier 2) height is h_2 = 14.1 ft. The purpose of having tiers of different heights is to trigger brace tensile yielding in one of the tiers first. A special concentrically braced frame system was selected.

The columns are made of wide-flange sections and oriented such that the out-of-plane bending moment occurs about the strong-axis of the section. A 23-ft horizontal strut is placed between tiers to prevent K-braced frame response and ensure the seismic load is appropriately transferred to the base through the truss action once the braces respond in the inelastic range.

Loading

The design loads for the selected building were determined in accordance with ASCE/SEI 7-16 *Minimum Design Loads and Associated Criteria for Buildings and Other Structures* (ASCE, 2016). Risk Category II was chosen, and it was assumed that the building is located on a Site Class C with a Seismic Design Category D. The gravity loads include the roof dead load DL = 21 psf, the exterior wall dead load WL = 10 psf, and a live load LL = 20 psf. The tributary area considered per column was calculated on the basis that steel roof trusses support the roof system between the exterior walls of the building. The resulting factored axial load at the top of each column was then calculated to be P_G = 56 kips.

The seismic load parameters include a response modification factor R = 6.0, overstrength factor Ω_o = 2, and a deflection amplification factor C_d = 5.0. The mapped risk-targeted Maximum Considered Earthquake (MCE_R) spectral response acceleration parameters, S_S = 1.362g and S_1 = 0.458g for short and 1.0-s periods, respectively, were used to obtain the design spectral response acceleration parameters S_{DS} = 0.908g and S_{D1} = 0.458g. The empirical fundamental period was calculated using C_t = 0.0488 and x = 0.75, which is equal to T_a = 0.25 s. The seismic design coefficient was then calculated as C_s = 0.15. The seismic weight of the building W is equal to 1,710 kips and was obtained from the roof dead load plus half of the exterior wall dead load. The equivalent lateral force procedure was used to calculate the frame seismic base shear V, which is the product of the seismic coefficient and the seismic weight. This force was amplified to account for accidental torsion, resulting in a seismic design base shear per frame equal to 71 kips.

FRAME DESIGN

Design of structural members was performed in accordance with the AISC *Specification for Structural Steel Buildings* (AISC, 2016b) and AISC *Seismic Provisions* (AISC, 2010; 2016a). This section summarizes the key design steps and member sizes for braces, columns, and the strut. The design of braces is presented once as the steps and requirements are the same for both the 2010 and 2016 designs. The column design is described for each braced frame individually. Design of the strut is presented once and differences between the 2010 and 2016 designs are highlighted. The frame drift check is then presented for each design.

Brace Design

The braces in both tiers were designed to resist the seismic load effects in tension and compression. The brace design compression force in Tier 1 is equal to $P_{r,b1}$ = 45 kips, which includes the seismic induced axial force $P_{E,b1}$ = 43 kips plus the gravity-induced axial force $P_{G,b1}$ = 2 kips. The design compression force of the Tier 2 brace is $P_{r,b2}$ = 44 kips, which similarly includes the seismic induced axial force $P_{E,b2}$ = 42 kips plus the gravity-induced axial force $P_{G,b2}$ = 2 kips. The braces are designed using square HSS members. Such members are commonly used in practice and are more efficient than singly symmetric sections as they have an identical radius of gyration about both principal axes of the section (Black et al., 1980). The braces are made of ASTM A1085 steel (ASTM, 2015a) with a yield stress F_y = 50 ksi and an expected yield stress R_yF_y = 62.5 ksi. Although use of the selected HSS grade was not common for the frames designed in 2010, the steel grade was kept the same for braces of both 2010 and 2016 designs to ease the comparison between the frames. Braces were designed such that they buckle out of the plane of the frame using a linear hinge zone in the gusset plate (Astaneh-Asl et al., 1985) as specified in the AISC *Seismic Design Manual* (AISC, 2018) to trigger out-of-plane buckling. An effective length of 0.45 times the total length of the brace, which is measured between the brace working points, was used in design to account for the lateral bracing provided by the brace acting in tension (Wakabayashi et al., 1974; Nakashima and Wakabayashi, 1992; El-Tayem and Goel, 1985, 1986; Sabelli and Hohbach, 1999). An identical HSS 3½×3½×¼ section was selected for braces of both tiers, even though the brace design forces and lengths are slightly different in the tiers. The brace design axial compression strengths were determined from the AISC *Specification* Chapter E to be $P_{c,b1}$ = 48 kips and $P_{c,b2}$ = 51 kips in Tiers 1 and 2, respectively. The selected section complies with the width-to-thickness ratio limit $b/t = 12 < 14$ as required for highly ductile members in AISC *Seismic Provisions* Section F2.5a. The global

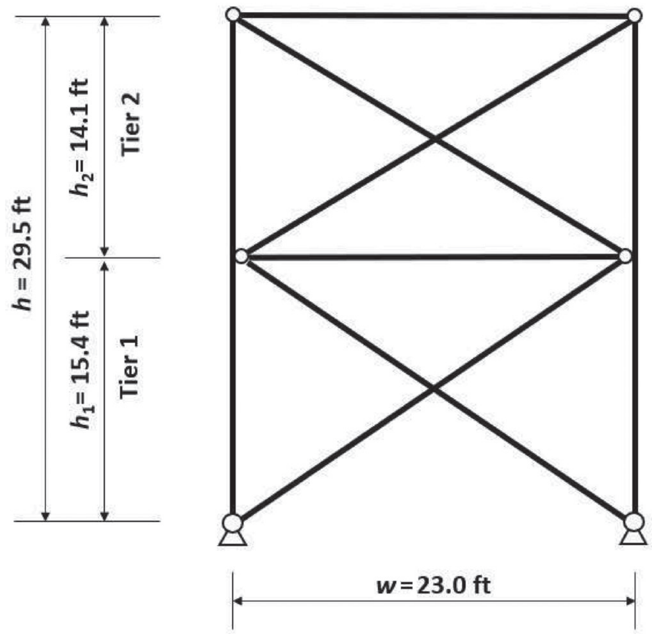

(a) Geometry of two-tiered SCBF selected for case study

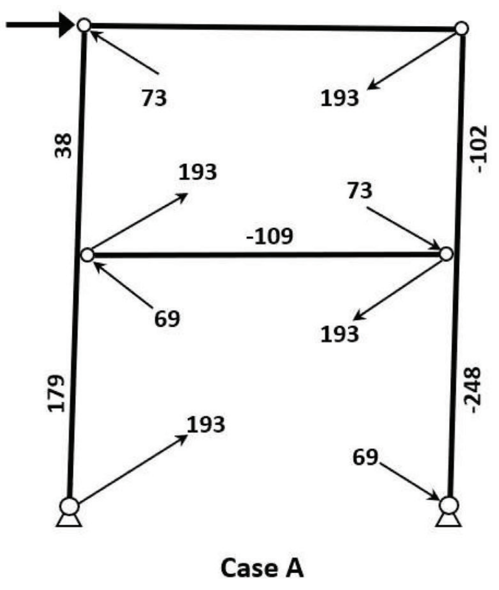

*(b) Analysis case A**

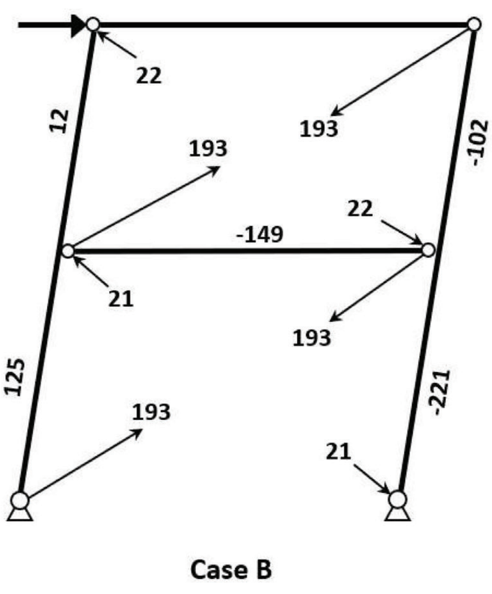

*(c) Analysis case B**

** No column bending moment considered.*

Fig. 4 (a–c). Geometry and internal member forces for the different seismic analyses of SCBFS (forces in kips).

slenderness ratios for braces in Tiers 1 and 2 are L/r = 113 and 110, respectively, which are less than the limit (i.e., 200) prescribed by AISC *Seismic Provisions* Section F2.5b.

Column Design

The columns of the selected braced frame were designed using two design methodologies, 2010 and 2016 AISC *Seismic Provisions*, to illustrate the design procedures and examine the seismic performance, in particular, the stability of columns.

2010 Design

The frame with the columns designed using the 2010 AISC *Seismic Provisions* is referred to as the 2010 design. The columns were designed to resist the axial compression force due to gravity loads $P_{G,c}$ = 51 kips plus the maximum axial

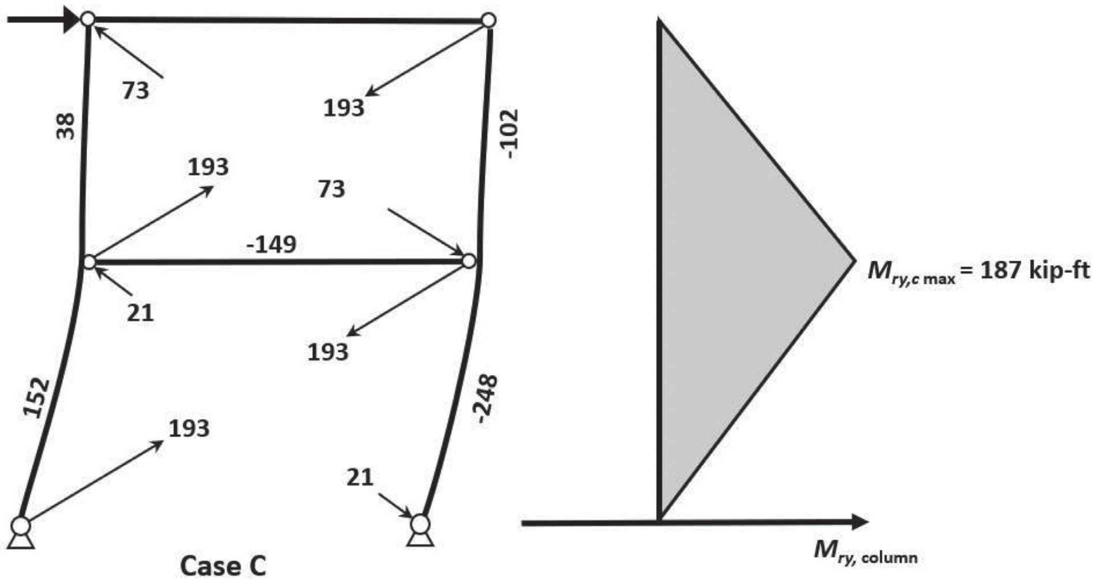

(d) Analysis case C with critical Tier 1

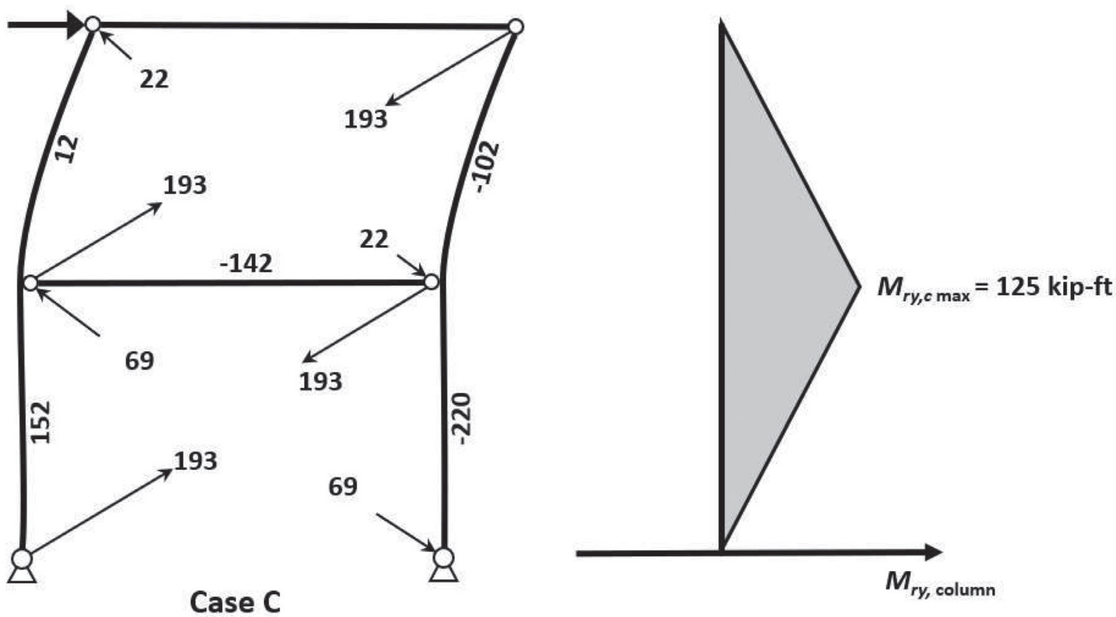

(e) Analysis case C with critical Tier 2

Fig. 4 (d–e). Geometry and internal member forces for the different seismic analyses of SCBFS (forces in kips).

load induced by the vertical components of brace forces when they reach their resistance in tension and compression. For the latter, two analysis cases are prescribed by the 2010 AISC *Seismic Provisions* Section F2.3 as shown in Figures 4(b) and 4(c). The maximum seismic axial compression force $P_{E,c}$ = 248 kips was obtained under analysis case A. The required column axial strength is $P_{r,c}$ = 299 kips. The columns are made of ASTM A992 steel (ASTM, 2015b) with a yield stress F_y = 50 ksi. To determine the flexural buckling resistance in the strong-axis and flexural-torsional buckling resistance of the column, the full-frame height was used, whereas, the weak-axis flexural buckling resistance was computed using the length of the column equal to the height of the first tier as the strut provides lateral support in the plane of the frame. The effective length factors K_x = 0.84, K_y = 0.80, and K_z = 1.0 were used to compute the column effective length factors in strong-axis, weak-axis, and torsion, respectively. The effective length factors for flexural buckling modes, K_x and K_y, were obtained using an Eigen buckling analysis of an individual column under the loads applied at the roof and tier levels using S-Frame software (S-Frame, 2017). A W16×45 column conforming to ASTM A992 Grade 50 steel (ASTM, 2015b) with yield stress F_y = 50 ksi was selected for the 2010 design as the lightest cross-section based solely on the axial demand since there are no flexural moments considered in design. The column design axial strength is equal to $P_{c,c}$ = 313 kips. Although in practice the effective length factors are generally taken equal to one, $K_x = K_y = K_z = 1.0$, in this study the effective length factors smaller than unity were used as allowed by the AISC *Specification* Appendix 7.2 to account for the beneficial effect of distributed axial loads on MT-CBF columns (Dalal, 1969). Had effective length factors equal to one been used in design, a W14×48 column section would have been chosen.

2016 Design

The 2016 design represents the frame with the columns designed using the 2016 AISC *Seismic Provisions*. The required strength of the columns was determined using the most critical combination of the axial compression force and bending moment obtained from analysis cases A, B, and C as shown in Figures 4(b)–4(e). One major difference between the 2010 and 2016 design is that analysis case C, which represents the progressive buckling and yielding of the braces as shown in Figure 3(c), is required in the 2016 design. Analysis case C resulted in the most critical demands on the columns as illustrated in Figure 4(d), including an axial compression force equal to $P_{r,c}$ = 299 kips due to the brace resistances plus the gravity load and an in-plane flexural bending moment $M_{ry,c}$ = 187 kip-ft caused by nonuniform yielding of the braces between two adjacent tiers. To calculate the in-plane bending moment in the columns, the critical tier was first identified by comparing the story shear resistance between the tiers: $V_{exp,1}$ = 218 kips < $V_{exp,2}$ = 228 kips. The shear resistance was obtained from the summation of the horizontal components of the brace resistances in tension and compression $V_{exp} = (T_{exp} + C_{exp})\cos\theta$, where θ is the angle between the brace and the horizontal plane. Comparing the shear resistances shows that Tier 1 has the least shear resistance and therefore is the critical tier. However, because the difference between the shear resistances is small, analysis case C was repeated assuming critical Tier 2 as shown in Figure 4(e). The case where the critical tier is Tier 1 resulted in the most critical combination of the axial compression force and flexural bending moment. The design in-plane bending moment of the column $M_{ry,c}$ is calculated using Equation 1 and the unbalanced brace story shear force ΔV_{br} as described in Imanpour et al. (2016b).

$$M_{ry,c} = \frac{\Delta V_{br} h_1}{1 + (h_1/h_2)} \tag{1}$$

where ΔV_{br} is the unbalanced brace story shear computed as follows:

$$\Delta V_{br} = \left(T_{exp} + C_{exp}\right)_2 \cos\theta_2 - \left(T_{exp} + C'_{exp}\right)_1 \cos\theta_1 \tag{2}$$

For the frame shown in Figure 4(d), the unbalanced brace story shear and design in-plane bending moment in the columns are equal to ΔV_{br} = 51 kips and $M_{ry,c}$ = 187 kip-ft (0.66 times the nominal plastic flexural strength in the weak-axis M_{py}), respectively. This was obtained assuming that the column is pinned in the plane of the frame at the roof and base levels.

As prescribed by the 2016 AISC *Seismic Provisions*, an additional out-of-plane bending moment demand equal to $M_{rx,c}$ = 4.2 kip-ft (0.007 times the nominal plastic flexural strength in the strong-axis M_{pxs}) was calculated, arising from the out-of-plane notional load applied at the tier level plus the brace out-of-plane buckling. The former effect was calculated by applying an out-of-plane horizontal notional load at the tier level that is 0.006 times the vertical component of the buckling strength of the Tier 2 brace; this force was amplified by multiplier B_1 = 1.16 to account for the P-δ effect. Multiplier B_1 was calculated using the method specified in 2016 AISC *Specification* Appendix 8.2. The latter effect need not exceed forces corresponding to the flexural resistance of the brace connections and was equal to $1.1R_yM_p/\alpha_s$, where R_y is the ratio of expected yield stress to the specified minimum yield stress, M_p is the corresponding plastic bending moment of the brace, and α_s is the LRFD force level adjustment factor taken equal to 1.0. A W12×96 column conforming to ASTM A992 Grade 50 steel was selected to carry the gravity plus seismic-induced forces for the frame of Figure 4(a). Note that had the effective length factors K_x, K_y, and K_z been set equal to 1.0, the column section would have remained unchanged. For the selected column, the axial strength, strong-axis flexural strength, and weak-axis flexural strength are $P_{c,c} = 1{,}020$ kips, $M_{cx,c} = 552$ kip-ft, and $M_{cy,c} = 255$ kip-ft, respectively. The column resistance was verified using the interaction equation given in AISC *Specification* Section H1.1:

$$\frac{P_{r,c}}{P_{c,c}} + \frac{8}{9}\left(\frac{M_{rx,c}}{M_{cx,c}} + \frac{M_{ry,c}}{M_{cy,c}}\right) \leq 1.0 \qquad \text{(from \textit{Spec}. Eq. H1-1a)}$$

$$\frac{299 \text{ kips}}{1{,}020 \text{ kips}} + \frac{8}{9}\left(\frac{4.20 \text{ kip-ft}}{552 \text{ kip-ft}} + \frac{187 \text{ kip-ft}}{255 \text{ kip-ft}}\right) \leq 1.0$$

$$0.95 < 1.0 \quad \textbf{o.k.}$$

Strut Design

The maximum axial compression force equal to $P_{r,s}$ = 149 kips was induced in the strut under analysis case B in Figure 4(c) for both the 2010 and 2016 designs. This analysis case corresponds to the brace loading scenario when the tension braces reach T_{exp} and C'_{exp} is developed in the compression braces of both tiers. As required by the 2016 AISC *Seismic Provisions*, when braces buckle out-of-plane, in addition to the axial compression force a flexural moment induced by brace buckling was considered in design; however, the torsional moment need not exceed the moment corresponding to the flexural resistance of the brace connections. Although the design forces between two designs are not identical, a W10×45 section made of ASTM A992 Grade 50 steel satisfies both designs. For the 2010 design, the strut was oriented such that the web is in the vertical plane; however, the web of the strut was placed in the horizontal plane for the 2016 design so that it can provide torsional bracing at the strut-to-column connections through its strong-axis moment capacity (Imanpour et al., 2016a; Stoakes and Fahnestock, 2014). This detail for the 2016 design was selected to satisfy the 2016 AISC *Seismic Provisions* requirement to torsionally brace the MT-CBF columns at the strut-to-column location.

Drift Checks

The story drift must be verified for both designs as specified in ASCE/SEI 7-16 (ASCE, 2016). The maximum story drift allowed by this standard is 2.5% for the structures in risk category II. The design story drift, Δ_d, was calculated by multiplying the elastic drift $\Delta_e = 0.12\%$ for the 2010 design and $\Delta_e = 0.11\%$ for the 2016 design by the deflection amplification factor $C_d = 5$ and divided by the importance factor I_e = 1: $C_d\, \Delta_e/I_e$ = 0.6% and 0.55% for the 2010 and 2016 designs, respectively. Both design story drifts satisfy the story drift limit prescribed by ASCE/SEI 7-16. Note that the elastic drift Δ_e can be calculated manually using structural analysis principles or using a structural analysis program under the design seismic force.

An additional drift limit is imposed by the 2016 AISC *Seismic Provisions* for individual braced tiers in MT-SCBFs to prevent premature brace failure due to excessive tier drifts (Tremblay et al., 2003; and Hsiao et al., 2013). It is required that the drift in each braced tier be limited to 2% of the tier height when the frame is subjected to the design story drift. This check was only performed for the 2016 design at the critical tier, which experiences the largest tier drift among the braced tiers. To calculate the critical tier drift, it was assumed that the tier drift is composed of two components: (1) the overall frame drift represented by a linear variation over the length of the frame Δ_F and (2) the distortion due to column bending caused by the unbalanced brace story shear ΔV_{br}. When the first tier is the critical tier, Equation 4 gives the first-tier drift:

$$\Delta_1 = \Delta_{F,1} + \left(\frac{V_{br}}{2}\right)\left(\frac{h_1 h_2^2}{3EI_c h}\right) \leq 2\% \tag{4}$$

where E = 29,000 ksi is the Young's modulus of steel, and I_c is the moment of inertia of the column about the weak-axis of the section.

The overall frame drift Δ_F is equal to the design story drift, Δ_d = 0.55%; therefore, $\Delta_{F,1}$ = 0.55%. To calculate the distortion due to column bending, the unbalanced brace story shear was calculated using the Case B forces shown in Figure 4(c), assuming that the compression braces in both tiers have experienced several inelastic cycles and reached their expected post-buckling capacity, while tension braces have reached their yield force and experienced significant elongations at least in one tier:

$$\begin{aligned}\Delta V_{br} &= \left(T_{exp} + C'_{exp}\right)_2 \cos\theta_2 - \left(T_{exp} + C'_{exp}\right)_1 \cos\theta_1 \\ &= (193 \text{ kips} + 22 \text{ kips})\cos 31.6° - \\ &\quad (193 \text{ kips} + 21 \text{ kips})\cos 33.9° \\ &= 5.40 \text{ kips}\end{aligned} \tag{5}$$

The drift in Tier 1 obtained using Equation 4 is equal to $\Delta_1 = 0.74\%$, which meets the 2% limit prescribed by the 2016 AISC *Seismic Provisions*. A similar check was performed assuming Tier 2 as the critical tier, which resulted in a critical tier drift equal to 0.76% and, therefore, satisfying the 2% limit as well. Thus, the selected column for the 2016 design satisfies the story drift and tier drift checks. Figures 5(a) and 5(b) show the final members selected for the 2010 and 2016 designs, respectively.

SEISMIC PERFORMANCE EVALUATION

Braced Frame Numerical Model

The three-dimensional finite element models of the two-tiered concentrically braced frames designed in accordance with the 2010 and 2016 AISC *Seismic Provisions* were developed using the *ABAQUS* program (ABAQUS, 2014).

The numerical model of the frame is shown in Figure 6. The frame connections were designed in accordance with the AISC *Seismic Design Manual* (AISC, 2018). All connections, excluding the column base connection, were included in the numerical models. Frame connections were designed as welded connections in accordance with AISC *Seismic Design Manual*; however, welds were not explicitly simulated in the numerical model; instead, connection plates and structural members were tied in their intersections. Three-dimensional deformable shell elements (S4R) were used to simulate braces, columns, struts, and connections. A finer mesh was used in the connection zones to better reproduce local effects. Material nonlinearity was incorporated through the Maxwell-Huber-Hencky-von Mises yield criterion with associated flow rule. The nonlinear kinematic/isotropic cyclic hardening model in *ABAQUS* was chosen to simulate the inelastic cyclic behavior of steel. The parameters used to define the hardening model were obtained from Suzuki and Lignos (2015). Geometric nonlinearities were incorporated in the models through the use of a large-displacement formulation. Young's modulus of elasticity and Poisson's ratio were assumed as 29,000 ksi and 0.3, respectively. The yield stress R_yF_y = 62.5 ksi and F_y = 50 ksi were assigned to the braces and other members, respectively.

The base of the columns and bottom-edge of the base gusset plates were constrained to a reference point at the center of the column. The three translational degrees-of-freedom (DOFs) along with the torsional degree-of-freedom were fixed at the reference point. The reference point was free to rotate in and out of the plane of the frame to simulate a pinned base condition of the braced frame columns. Similarly, at the top of each column, the web and flanges were constrained to a reference point at the middle of the web of the column. These reference points at the top of the columns were restrained from out-of-plane movement and twist. The reference points at the top were free to move in the plane of the frame and rotate in and out of the plane of the frame.

Initial geometric imperfections corresponding to the first buckling mode of the members, which were obtained from an eigenvalue buckling analysis, were assigned to columns and braces. The amplitude of the initial geometric imperfection was taken equal to 1/1000 times the unbraced length of the member in the direction of buckling (AISC, 2016c). For the columns, the total height of the frame was used for the out-of-plane direction, and the tier heights were used for the amplitudes in the plane of the frame. For the braces, the imperfections were only considered in the out-of-plane direction within the half of the brace length. Initial residual stresses were incorporated in wide-flange sections based on the pattern proposed by Galambos and Ketter (1958). A leaning column was also included in the model to account for large P-Δ effects. The leaning column was simulated using a deformable wire element and pin connected at its base and top. The in-plane horizontal displacement of the leaning column was constrained to the lateral displacement of the braced frame at the roof level. Additional information on the numerical model development and calibration can be found in Cano (2019).

Inertial forces developed at the roof level were reproduced using two point masses at the top end of the braced frame columns. The masses represent the weight equal to

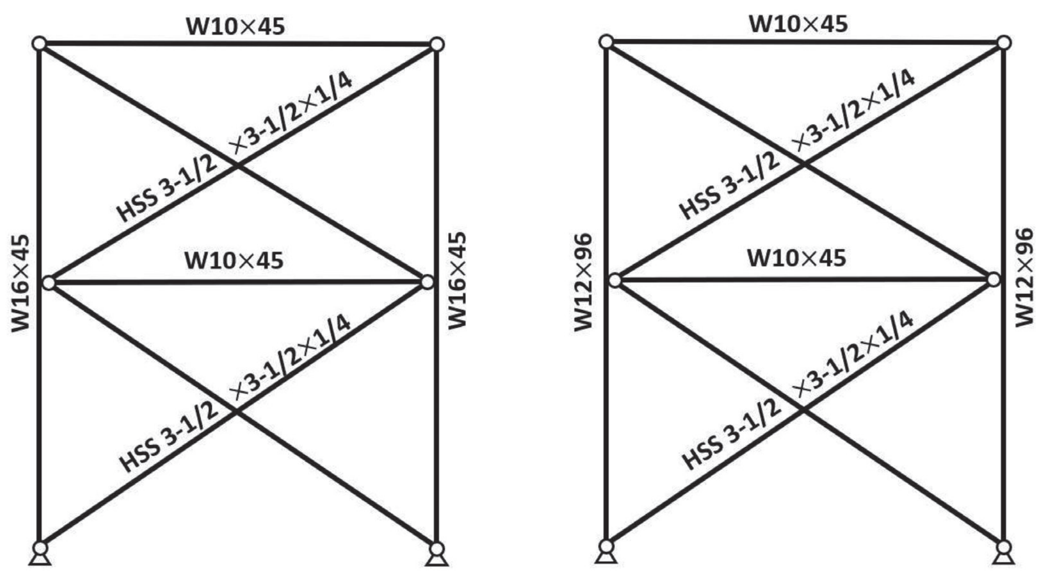

(a) 2010 design *(b) 2016 design*

Fig. 5. Selected members for two-tiered SCBF.

one-eighth of the total building seismic weight. The masses corresponding to the self-weight of the strut, roof beam, and connections were assigned as mass densities. However, only 0.1% of the mass density corresponding to the braces and columns was input in the mass definition to overcome the overshoot effect in the prediction of brace buckling response (Kazemzadeh Azad et al., 2018). Damping was defined using the Rayleigh's damping method to generate the damping forces under dynamic loading.

Nonlinear static (pushover) and dynamic analyses were performed on both 2010 and 2016 models. Each analysis was carried out in two steps. A gravity load of 51 kips was applied at the top end of each column in the first step using the static/general procedure. The gravity load equal to 675 kips corresponding to the adjacent gravity columns in the selected building was also applied at the top end of the leaning column in the same step. Once the gravity loads were applied, the lateral seismic load was applied. For the nonlinear static analysis, the frame was subjected to a cyclic horizontal displacement history at its roof level using a similar static/general procedure. For the nonlinear dynamic analysis, a set of ground motion accelerations were applied to the base of the frame and leaning column in the horizontal direction. Note that the inertia masses were only included in the dynamic analysis. To perform the dynamic analysis, the dynamic implicit procedure was selected, which uses the Newton-Raphson method to solve the nonlinear dynamic equilibrium.

Loading History for Nonlinear Static Analysis

Figure 7 shows the horizontal displacement history applied to the frames at the roof level. The displacement history consists of 14 cycles in which the first 10 cycles were obtained from the displacement history prescribed for prequalification of buckling restrained braces (BRBs) in 2016 AISC *Seismic Provisions* Appendix K plus four additional cycles: two cycles with the peak displacement corresponding to three times the frame design story drift and the last two cycles corresponding to four times the design story drift. The largest displacement cycle was selected to reproduce the maximum roof displacement observed in the dynamic analysis of the frame (see Table 1). In Figure 7, δ_y is the story drift corresponding to brace tensile yielding, and $C_d\delta_e$ is the frame design story drift per ASCE/SEI 7-16.

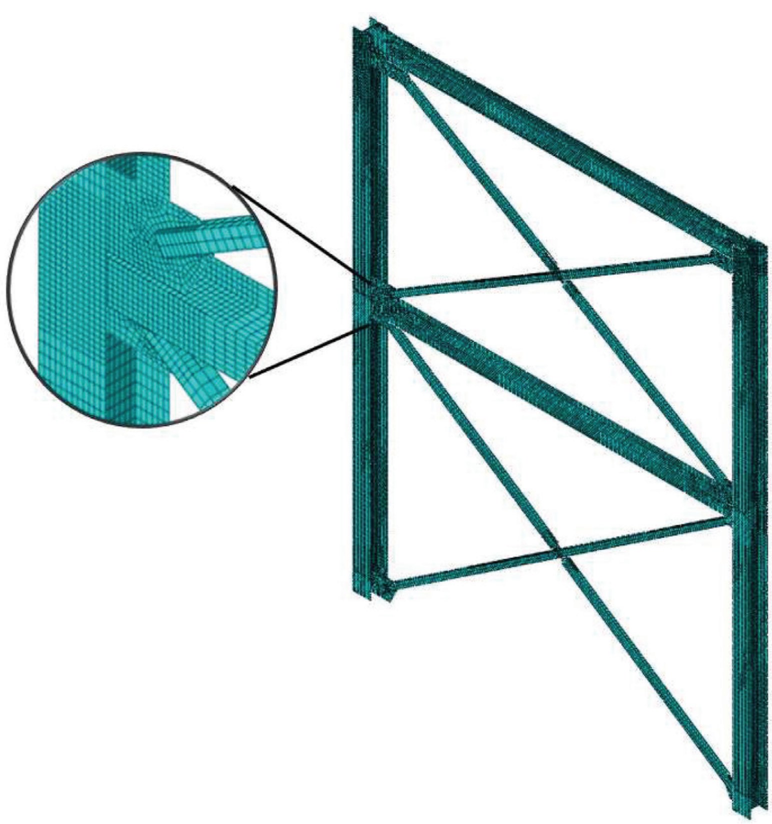

Fig. 6. Finite element model of the two-tiered concentrically brace frame (leaning column not shown for clarity).

Ground Motion Acceleration for Nonlinear Dynamic Analysis

The set of ground motion accelerations used to perform the dynamic analysis comprises the horizontal component of 40 historical ground motions. The ground motion records were selected and scaled using the method proposed by Dehghani and Tremblay (2016) to match, on average, the code-prescribed MCE_R response spectra as given in ASCE 7 at the fundamental period of the braced frame. The selection and scaling methods are described in detail in Dehghani (2016). The ensemble contains 14 records representing crustal earthquakes (0–185 miles), 21 records representing interplate earthquakes (45–185 miles deep), and 5 records representing in-slab earthquakes (185–440 miles).

Nonlinear Static Analysis Results

The results obtained from the nonlinear static (pushover) analysis of the 2010 and 2016 designs are presented in this section. Figures 8(a) and 8(b) show the drift demands in both tiers for the 2010 and 2016 designs, respectively. For both designs, the drifts in both braced tiers are nearly identical through the first six cycles before the story drift reaches 0.6%. Brace buckling took place in both tiers in the seventh cycle. Brace yielding was then initiated in the critical Tier 1, as expected in design. In the 2010 design, however, the subsequent brace elongation in tension led to a significantly larger drift in this tier compared to Tier 2, which remained essentially elastic through the entire analysis. The nonuniform distribution of drift demands was observed in the subsequent cycle, which eventually led to column instability in the first-tier segment of the right-hand-side (RHS) column of the 2010 design. Column buckling occurred under the combination of large in-plane bending moment and axial compression force demands. Figure 9(a) shows the deformed frame shape at the initiation of column buckling. The analysis stopped just at the column buckling due to numerical convergence issues at 2.0% story drift.

The response of the 2016 design was significantly different than the 2010 counterpart. Brace tensile yielding developed in Tier 2 at 0.76% story drift, which reduced the nonuniformity of lateral inelastic deformations along the frame height. As shown in Figure 8(b), inelastic frame lateral deformations were distributed more uniformly between the tiers. Nevertheless, tier drift in critical Tier 1 was still higher than the one in noncritical Tier 2. No column instability was observed in the 2016 design. The frame deformed shape at the maximum story drift applied (i.e., 2.1%) is shown in Figure 9(b).

The brace axial forces in both tiers were normalized by the maximum expected tensile strength, AR_yF_y where A is the cross-sectional area of the brace and R_yF_y is the expected yield stress, and plotted against the tier drift in Figures 10(a) and 10(b) and Figures 10(c) and 10(d) for 2010 and 2016 designs, respectively. For the 2010 design, the tension brace in Tier 2 remained essentially elastic. Although the compression brace experienced buckling in compression, the buckling capacity was not significantly reduced; however, the braces in Tier 1 underwent severe inelastic deformations due to severe buckling and yielding. In contrast, the braces

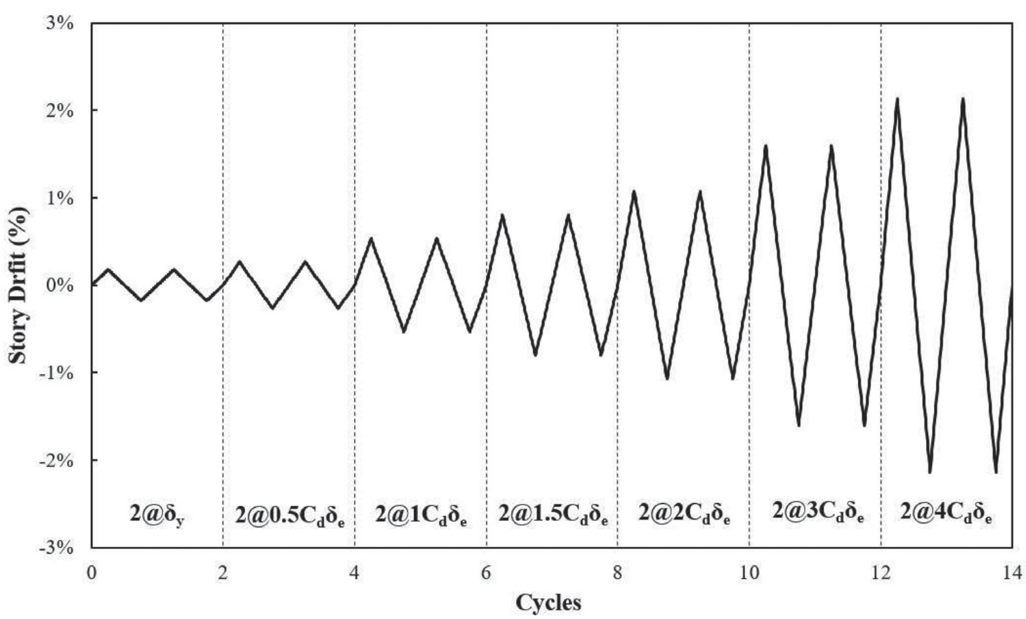

Fig. 7. Horizontal displacement history.

in both tiers of the 2016 design contributed to the inelastic response of the frame through yielding and buckling as shown in Figures 10(c) and 10(d).

Column in-plane bending moments recorded just below the brace-to-column connection were plotted against the story drift for 2010 and 2016 designs in Figures 11(a) and 11(b), respectively, to determine how the differential tier drifts can affect the bending moment demand on the column. The results are only presented for the critical RHS column, which is in compression when column buckling takes place in the 2010 design. The moments were normalized by the weak-axis plastic moment M_{py} of the corresponding section. The maximum normalized moment demand in the frame designed using the 2010 and 2016 AISC *Seismic Provisions* are 0.34 and 0.33, respectively. In 2016 design, the tension brace in Tier 2 yields at approximately 0.7% story drift, and the columns begins to straighten, which, combined with large-P-Δ effects, led to a nearly constant in-plane moment for the story drift exceeding 0.7% as shown in Figure 11(b). This is due to the combination of the moment arising from the decrease of the unbalanced brace story shear plus the P-Δ effects on the RHS column when it is under compression. It was also found that the design in-plane bending moment as per the 2016 AISC *Seismic Provisions* was largely overestimated ($0.66M_{py}$ vs. $0.33M_{py}$).

Column out-of-plane bending moments recorded just below the brace-to-column connection are plotted against the story drift for 2010 and 2016 designs in Figure 11(c) and 11(d), respectively. The moments were normalized by the strong-axis plastic moment M_{px} of the corresponding section. The columns of the 2010 and 2016 designs experienced a maximum out-of-plane demand of 17.0 kip-ft ($0.05M_{px}$) and 18.4 kip-ft ($0.03M_{px}$), respectively. The maximum out-of-plane bending moment obtained for the 2016 design significantly exceeded the design value specified in the 2016 AISC *Seismic Provisions* ($0.007M_{px}$ vs. $0.03M_{px}$). However, it was observed that the maximum in-plane and out-of-plane moments generally do not co-exist. The maximum in-plane moments are experienced at story drifts that occur when the brace tensile yielding is initiated in the noncritical tier or higher (i.e., >0.7% story drift), but the out-of-plane moment value is driven by the compression brace force meeting the column at the tier level, and its maximum is achieved when the compression brace in the noncritical tier begins to buckle, which occurs at relatively small story drift.

The results obtained from the nonlinear static analysis suggest that the strength and stability of the column designed in accordance with the 2016 AISC *Seismic Provisions* is satisfactory even though the in-plane and out-of-plane bending demands are not accurately estimated in design. The overestimation of the in-plane moment demand can be attributed to the fact that the demand is calculated with a conservative assumption of brace expected strengths, which agrees with the other brace loading analysis cases [see Figures 2(a) and 2(b)] prescribed by the standard for multi-story SCBFs. The underestimation of the out-of-plane moment demand is not expected to have a significant impact on design due to relatively low moment demands compared to a large strong-axis moment capacity provided by the column selected to primarily resist the axial compression force and large weak-axis bending moment. For comparison, the interaction ratio is recalculated to be 0.62 using the measured column forces from the numerical analysis, which is lower than 0.95 obtained using design values, thus confirming the adequacy of the new column design requirements specified in 2016 AISC *Seismic Provisions*.

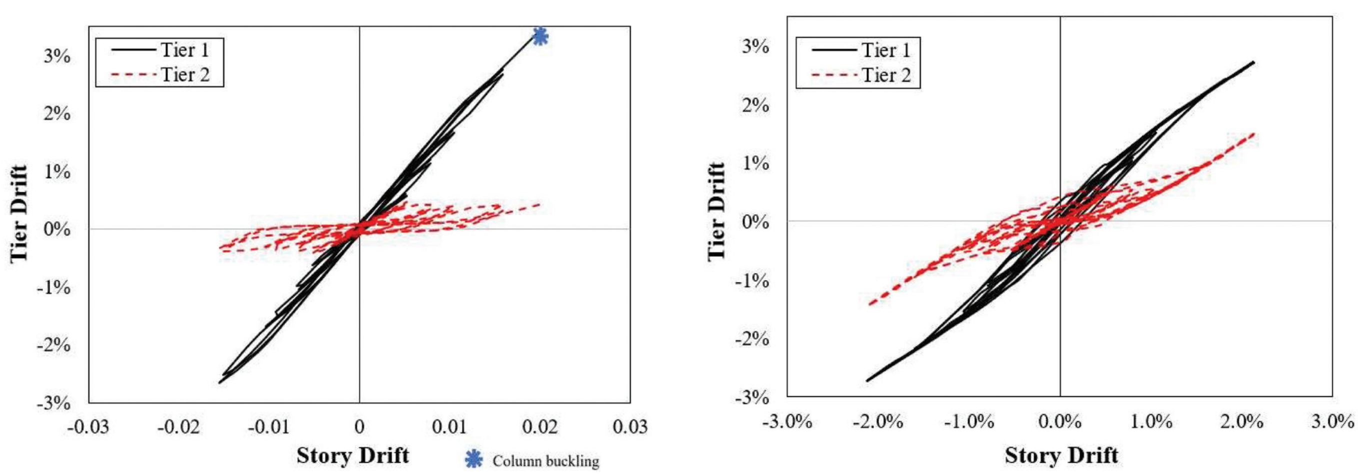

(a) 2010 design *(b) 2016 design*

Fig. 8. Tier drift versus story drift.

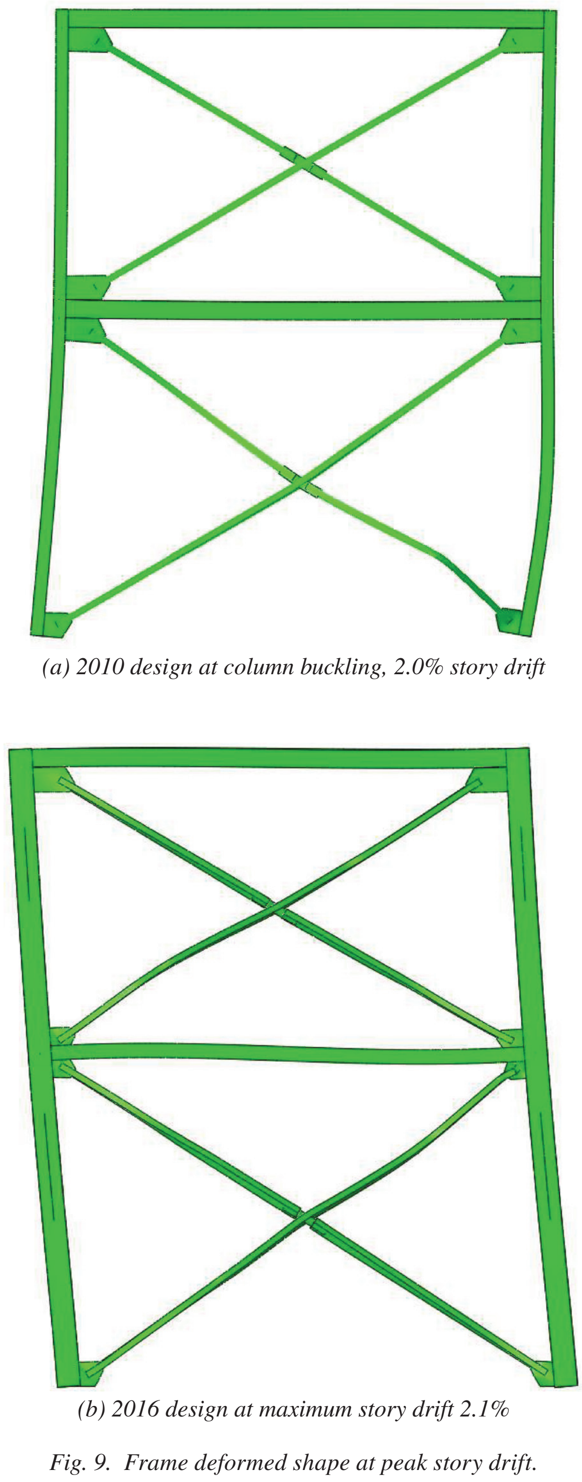

(a) 2010 design at column buckling, 2.0% story drift

(b) 2016 design at maximum story drift 2.1%

Fig. 9. Frame deformed shape at peak story drift.

Nonlinear Dynamic Analysis Results

The results obtained from the nonlinear dynamic analysis of the 2010 and 2016 designs under 40 ground motion records are presented in this section.

2010 Design Overall Behavior

Column instability similar to the one observed using the static analysis method was observed for the 2010 design under 13 ground motion records out of the 40 ground motions analyzed. Column buckling triggered dynamic instability and led to frame collapse in all 13 cases. Figure 12 shows an example of the frame collapse under the 1994 Northridge ground motion record. Examining the results of the collapsed cases showed that the left-hand-side (LHS) column buckled upon reaching lower story drifts in comparison to the RHS column due to the direction of initial geometric imperfections, which favored the in-plane buckling of the LHS column. The in-plane flexural buckling was observed first with a limited twist; the instability mode then changed to out-of-plane buckling due to the lack of out-of-plane support, resulting in a flexural-torsional buckling mode.

The statistics of the NonLinear Response History (NLRH) analysis results were used to evaluate the seismic response of the frames. Table 1 presents the results for the story drift, story drift ratio normalized by the design story drift $C_d\Delta_e$, drifts in Tiers 1 and 2, and drift ratios in Tiers 1 and 2 normalized by the story drift. For each parameter, the maximum, minimum, median and 84th percentile of the maximum recorded value under each ground motion are given. Note that the maximum, median, as well as the 84th percentile values were computed based on the ground motion records where the frame did not collapse. The story drifts range between 0.5% and 2.2% with a median value of 1.1%. Comparing the tier drift results for the non-collapse cases shows that drift in Tier 1 is approximately three times that of Tier 2, which confirms the finding of the static analysis and that brace tensile yielding only occurred in the critical tier.

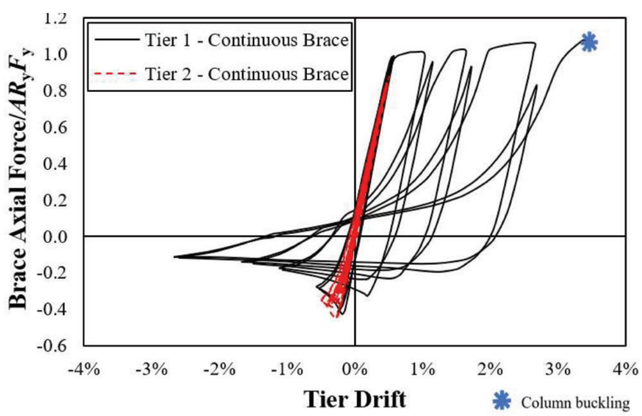

(a) 2010 design continuous braces

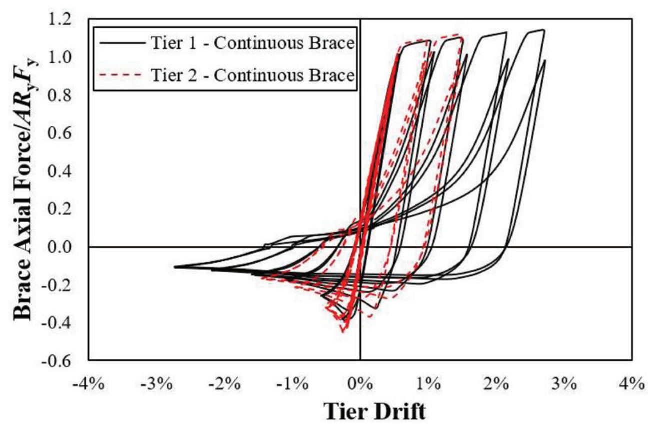

(b) 2016 design continuous braces

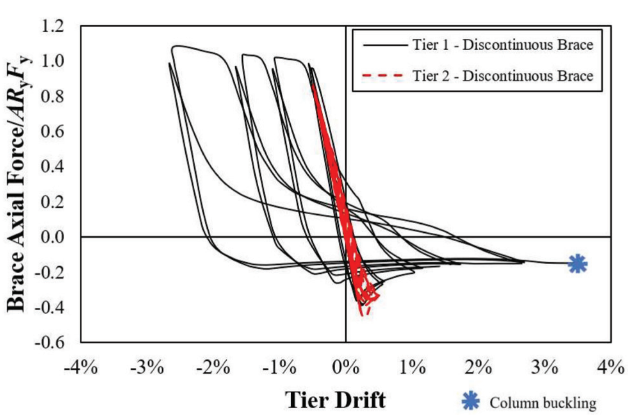

(c) 2010 design discontinuous braces

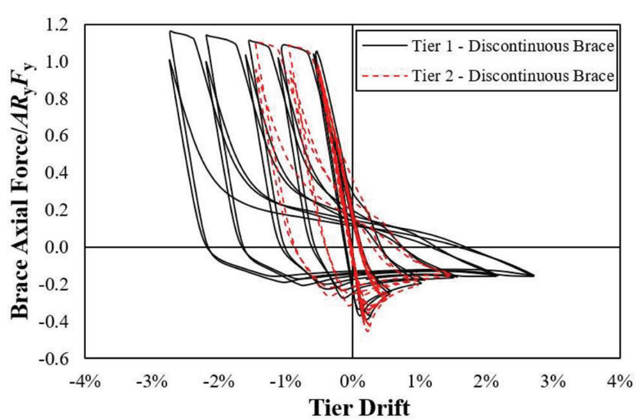

(d) 2016 design discontinuous braces

Fig. 10. Normalized brace axial forces.

Table 1. Dynamic Analysis Statistics for Drift Response							
		Story Drift		Tier 1 Drift	Tier 2 Drift		
	Parameters	Δ	$\Delta / C_d \Delta_e$	Δ_1	Δ_2	Δ_1 / Δ	Δ_2 / Δ
2010 Design	Minimum	0.5%	0.8	0.5%	0.5%	1.0	1.0
	Maximum	2.2%	3.6	3.6%	0.6%	1.7	0.3
	Median	1.1%	1.9	1.7%	0.5%	1.5	0.4
	84th percentile	1.5%	2.5	2.4%	0.5%	1.6	0.4
2016 Design	Minimum	0.5%	0.9	0.5%	0.5%	1.0	1.0
	Maximum	2.6%	4.7	3.3%	1.9%	1.6	0.7
	Median	1.4%	2.5	2.0%	0.7%	1.4	0.5
	84th percentile	1.9%	3.5	2.6%	1.3%	1.5	0.7

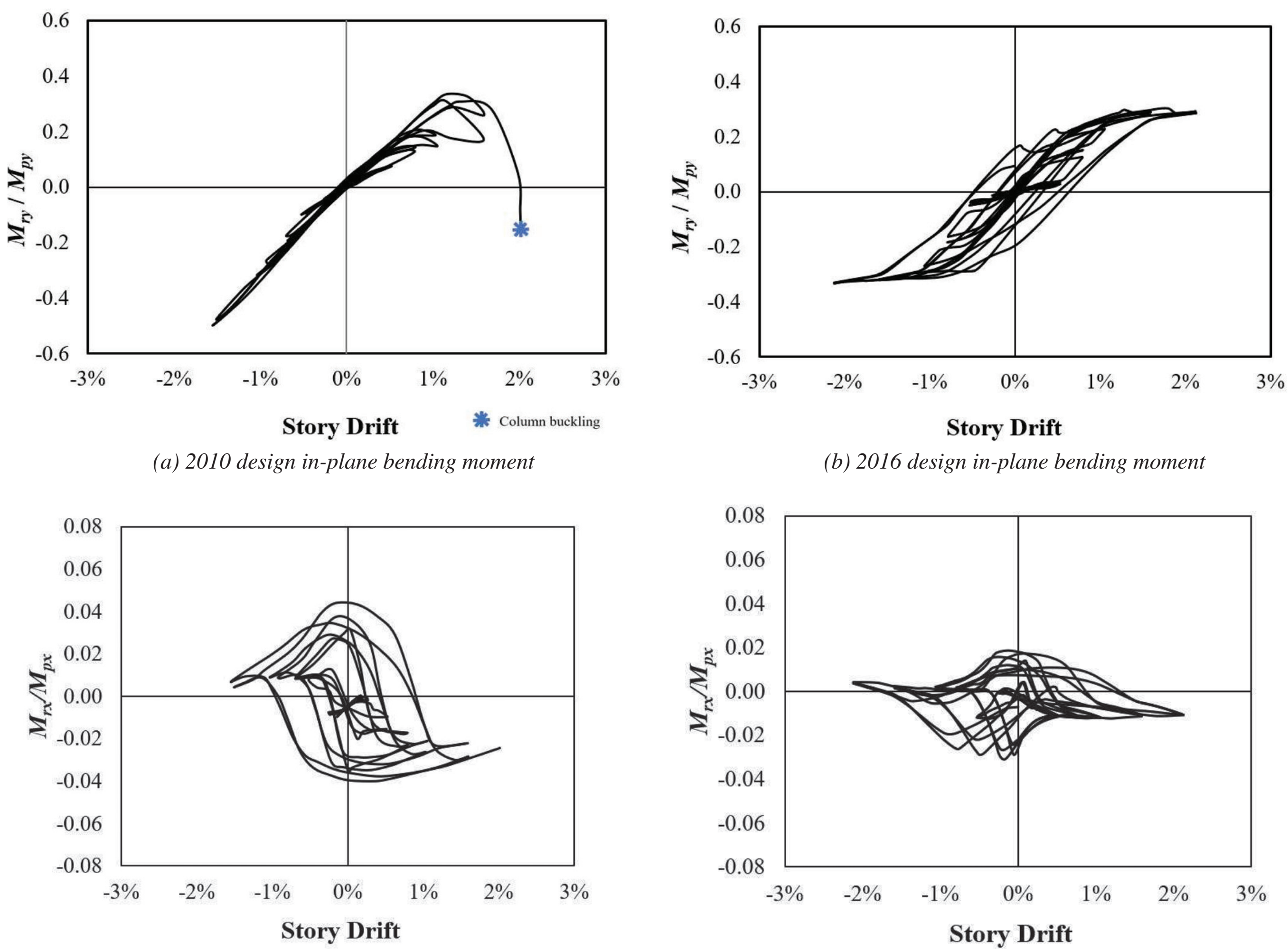

(a) 2010 design in-plane bending moment

(b) 2016 design in-plane bending moment

(c) 2010 design out-of-plane bending moment

(d) 2016 design out-of-plane bending moment

Fig. 11. RHS column moment demands.

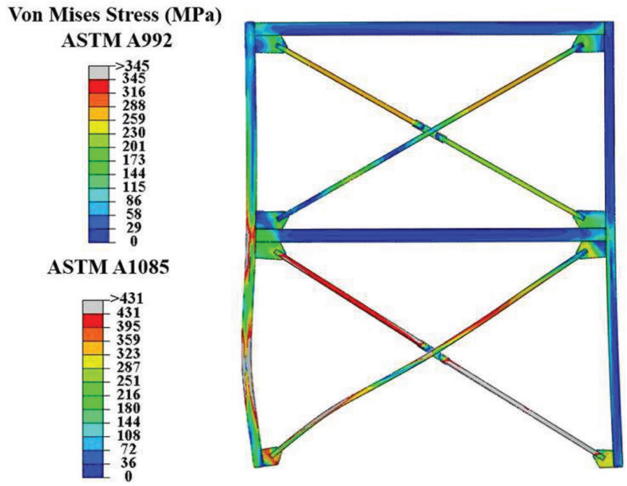

(a) Onset of LHS column buckling at t = *4.70 sec and story drift of 1.7%*

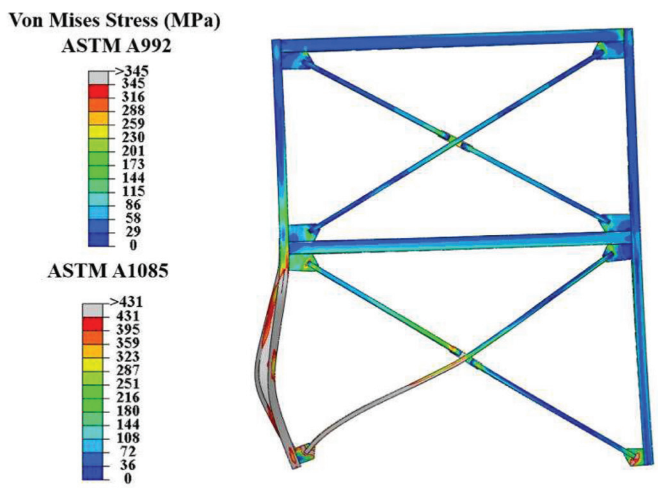

(b) LHS column buckling at t = *5.38 sec*

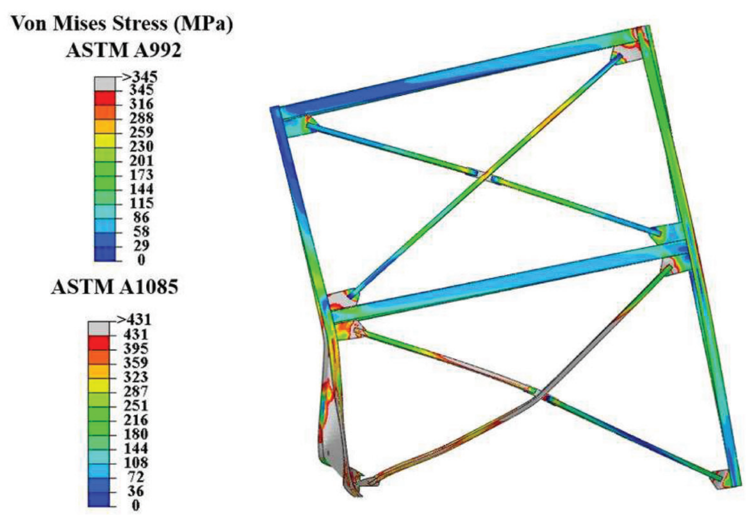

(c) Frame collapse at t = *5.49 sec*

Fig. 12. 2010 frame deformed shape under 1994 Northridge record.

	Table 2. Dynamic Analysis Statistics for Column Demands						
	Parameters	M_{ry}/M_{py}	$M_{ry}/M_{ry,design}$	M_{rx}/M_{px}	$M_{rx}/M_{rx,design}$	P_r/P_n	$P_r/P_{r,design}$
2010 Design	Minimum	0.04	–	0.01	–	0.86	1.00
	Maximum	0.31	–	0.10	–	0.92	1.07
	Median	0.18	–	0.06	–	0.90	1.04
	84th percentile	0.28	–	0.08	–	0.91	1.06
2016 Design	Minimum	0.01	0.01	0.01	0.51	0.25	0.94
	Maximum	0.41	0.61	0.06	2.32	0.27	1.02
	Median	0.30	0.46	0.04	1.63	0.26	0.99
	84th percentile	0.35	0.53	0.05	1.96	0.26	1.00

2016 Design Overall Behavior

The results obtained for the 2016 design indicated that neither column buckling nor frame instability occurs under any of the 40 ground motion records. The summary of the frame displacement response is presented in Table 1. The median story drift is 1.4%, 2.5 times higher than the design story drift. The maximum story drift of 2.6% occurred under the 1979 Montenegro, Yugoslavia, earthquake. Note that the median story drift for the 2016 frame appears higher than the 2010 design; however, this is because the collapsed cases are not included in the calculation of median for the 2010 design.

The results of the tier drifts for the 2016 frame indicate that the tension brace in noncritical Tier 2 yields under the majority of the ground motion records, which significantly improved the distribution of inelastic lateral deformations over the height of the selected braced frame. Although the critical tier drift exceeded the limit prescribed by 2016 AISC *Seismic Provisions* (i.e., 2.0%) under a few major earthquakes, the median value of the critical tier drift 2.0% suggests that the stiffness design requirements specified in the 2016 AISC *Seismic Provisions* on average lead to a satisfactory drift response.

2010 Design Column Behavior

The statistics of the maximum column demands, including bending moments and axial forces for the 2010 and 2016 designs, are given in Table 2. The moment values were normalized by the corresponding plastic moment M_p (x and y are the strong and weak axis of the section, respectively), and axial forces were normalized by the nominal compressive strength. For the 2010 design, the axial forces were compared against the design value only because there were no moments used in design to compare against flexural demands. For the 2016 design, both the flexural moments and axial forces were compared against the designed values. Column moment demands were recorded for each ground motion just below the brace-to-column connection in Tier 1.

The results obtained for the 2010 frame indicate a high axial compression force that matches the design axial compression load is induced in the columns. Column in-plane and out-of-plane moments were not significantly large because the statistics only encompasses the noncollapse cases.

2016 Design Column Behavior

The axial force and moment values in the 2016 design show that the column capacity is shared between the axial force and biaxial bending moments as expected in design. However, the measured in-plane bending moment is lower than the value obtained using the current AISC *Seismic Provisions* because (1) brace tensile yielding does not occur under some of the ground motion records, and (2) the compression brace forces assumed in design to compute the unbalanced brace story shear (C'_{exp} in the critical tier and C_{exp} in noncritical tier) were found to be higher than C'_{exp} in the critical tier, due to the difference between the observed strength degradation at the post-buckling range and that expected in the standard to determine C'_{exp}, and lower than C_{exp} in the noncritical tier, due to slight strength degradation after achieving brace buckling.

Out-of-plane moments for the 2016 frame exceeded the design out-of-plane moment as per the 2016 AISC *Seismic Provisions* in 35 out of 40 cases with a median $M_{rx}/M_{rx,design}$ value of 1.63. The maximum out-of-plane moment tends to occur when the braces reach their maximum buckling capacity and generally do not coincide with the maximum in-plane moment. The out-of-plane moment was investigated further by differentiating the contributing components including (tension and compression) brace forces, strut forces, gusset plate plastic moments, and P-δ effects. It was found that the out-of-plane moment induced by the out-of-plane component of the brace forces and the P-δ effects are the key contributors to the out-of-plane bending moment of the compression column. The contribution from the braces on the out-of-plane moment of the columns was found not only to be caused by the buckled compression braces, but also by the tension braces. This is because residual plastic deformations developed upon brace out-of-plane buckling result in an elongated brace in the subsequent tension cycle that creates out-of-plane forces on the column. However, such out-of-plane deformations in the tension brace were considerably smaller than those in the compression brace since the brace tends to straighten under the tension load. The results of the NLRH analyses showed that although the moment demands are not accurately predicted, the stability and strength of the column designed in accordance with the 2016 AISC *Seismic Provisions* are satisfactory.

CONCLUSIONS

This paper presents the seismic response of steel multi-tiered special concentrically braced frames designed in accordance with the 2010 and 2016 AISC *Seismic Provisions*. A detailed nonlinear finite element model of a two-tiered special concentrically braced frame capable of simulating the brace inelastic response and column instability modes was developed. This numerical model was analyzed under cyclic displacement demands and earthquake accelerations to assess the frame nonlinear lateral response and evaluate the column moment demands prescribed by the latest edition of the AISC *Seismic Provisions*. The main findings of this study are summarized as follows:

- The seismic response of both 2010 and 2016 frames predicted using cyclic nonlinear static analysis agrees well with that predicted using the nonlinear dynamic analysis.
- Inelastic frame deformations tend to concentrate in one of the braced tiers in the frame designed in accordance with the 2010 AISC *Seismic Provisions*. Such nonuniform lateral response led to column instability in the first-tier segment for the frame.
- Column instability in the 2010 design is influenced by the direction of the initial geometric imperfection assigned in the plane of the frame. Because the column instability is initiated by flexural buckling mode in the plane of the frame within a tier, the column with the initial geometric imperfection aligned with the direction of lateral displacement demand is more prone to instability.
- The seismic response of the frame designed in accordance with the 2016 AISC *Seismic Provisions*, where the columns were sized to resist additional in-plane and out-of-plane bending moments, was significantly improved compared to the frame designed to the 2010 AISC *Seismic Provisions*.
- Neither yielding nor instability occurred in the columns designed in accordance with the 2016 AISC *Seismic Provisions*.
- The column designed using the 2016 AISC *Seismic Provisions* possesses sufficient stiffness to trigger yielding in the noncritical tier under large story drifts, which allows for better distribution of inelastic frame deformations over the height of the frame.
- The median value of the peak tier drifts for the 2016 design as obtained from the nonlinear response history analyses is within the limit prescribed by the 2016 AISC *Seismic Provisions.*
- The results of nonlinear response history analyses performed on the 2016 design confirmed that the column axial force demand is appropriately predicted, the in-plane bending moment demand of the column is overestimated, and the out-of-plane bending moment demand of the column is underestimated. However, the underestimation of the out-of-plane moment demand did not have a detrimental effect on the frame seismic response.

Future numerical simulations should investigate a large number of multi-tiered steel concentrically braced frames with different geometries to further validate the 2016 AISC *Seismic Provisions* and improve further if necessary. In particular, the results of such studies can be used to evaluate torsional and out-of-plane demands of the column. Furthermore, the results obtained from the present numerical simulations should be validated using full-scale experimental tests on two-tiered concentrically braced frames once available.

ACKNOWLEDGMENTS

The authors wish to express their sincere appreciation to the Natural Sciences and Engineering Research Council (NSERC) of Canada and the Faculty of Engineering of the University of Alberta for the financial support provided for this study. The authors wish to thank Dr. Morteza Dehghani and Prof. Robert Tremblay of Polytechnique Montreal for sharing the ground motion acceleration data. Support provided by the CISC Centre for Steel Structures Education and Research (Steel Centre) at the University of Alberta is greatly acknowledged. The authors also wish to thank the reviewers for their cogent and constructive comments, which led to an improvement on the quality of the paper.

REFERENCES

ABAQUS (2014), Dassault Systèmes, Waltham, Mass.

AISC (2010), *Seismic Provisions for Structural Steel Buildings*, ANSI/AISC 341-10, American Institute of Steel Construction, Chicago, Ill.

AISC (2016a), *Seismic Provisions for Structural Steel Buildings*, ANSI/AISC 341-16, American Institute of Steel Construction, Chicago, Ill.

AISC (2016b), *Specification for Structural Steel Buildings*, ANSI/AISC 360-16, American Institute of Steel Construction, Chicago, Ill.

AISC (2016c), *Code of Standard Practice for Steel Buildings and Bridges*, ANSI/AISC 303-16, American Institute of Steel Construction, Chicago, Ill.

AISC (2018), *Seismic Design Manual*. American Institute of Steel Construction, Chicago, Ill.

ASCE (2016), *Minimum Design Loads for Buildings and Other Structures*, ASCE/SEI 7-16, American Society of Civil Engineers.

Astaneh-Asl, A., Goel, S.C., and Hanson, R.D. (1985), "Cyclic Out-of-Plane Buckling of Double-Angle Bracing," *Journal of Structural Engineering,* ASCE, Vol. 111, No. 5, pp. 1,135–1,153.

ASTM (2015a)*, Standard Specification for Cold-Formed Welded Carbon Steel Hollow Structural Sections (HSS),* A1085/A1085M-15, ASTM International, West Conshohocken, Pa.

ASTM (2015b), *Standard Specification for Structural Steel Shapes*, A992/A992M-11, ASTM International, West Conshohocken, Pa.

Black, R. Gary, Wenger, W.A., and Popov, E.P. (1980), "Inelastic Buckling of Steel Struts under Cyclic Load Reversal," Earthquake Engineering Research Center, University of California, Berkely, Calif.

Cano, P.A. and Imanpour, A. (2018), "Evaluation of Seismic Design Methods for Steel Multi-Tiered Special Concentrically Braced Frames," *Proceedings Structural Stability Research Council Annual Stability Conference 2018* (April 10–13). Baltimore, Md.

Cano, P.A. (2019), *Evaluation of the Seismic Design Methods for Steel Multi-Tiered Concentrically Braced Frames*, Master's Thesis, University of Alberta.

Cano, P.A. and Imanpour, A. (2019), "Dynamic Analysis of Steel Multi-Tiered Special Concentrically Braced Frames," *Structures Congress 2019,* Orlando, Fla. April 24–27, pp. 99–112.

Dalal, S. T. (1969), "Some Non-Conventional Cases of Column Design," *Engineering Journal,* AISC, Vol. 6, No. 1, pp. 28–39.

Dehghani, M. (2016), *Seismic Design and Qualification of All-Steel Buckling-Restrained Braced Frames for Canadian Applications*, Dissertation from Ecole Polytechnique Montreal, Order No. 10806518, Ecole Polytechnique, Montreal, Canada.

Dehghani, M. and Tremblay, R. (2016), "Robust Period-Independent Ground Motion Selection and Scaling for Effective Seismic Design and Assessment," *Journal of Earthquake Engineering*, Vol. 20, No. 2, pp. 185–218. DOI: 10.1080/13632469.2015.1051635.

El-Tayem, A.A. and Goel, S.C. (1985), "Cyclic Behavior of Angle X-Bracing with Welded Connections," Research Report No. UMCE 85-4, University of Michigan, Ann Arbor, Mich.

El-Tayem, A.A. and Goel, S.C. (1986), "Effective Length Factor for the Design of X-Bracing Systems," *Engineering Journal,* AISC, Vol. 24, No. 1, pp. 41–45.

Galambos, T.V. and Ketter, R.L. (1958), "Columns under Combined Bending and Thrust," Report 205A.21, Fritz Engineering Laboratory, Bethlehem, Pa.

Hsiao, P-C., Lehman, D.E., and Roeder, C.W. (2013), "A Model to Simulate Special Concentrically Braced Frames Beyond Brace Fracture," *Earthquake Engineering and Structural Dynamics*, Vol. 42, pp. 183–200.

Imanpour, A., Stoakes, C., Tremblay, R., Fahnestock, L., and Davaran, A. (2013), "Seismic Stability Response of Columns in Multi-Tiered Braced Steel Frames for Industrial Applications," *Proceedings of the 2013 SEI Structures Congress,* pp. 2,650–2,661.

Imanpour, A. and Tremblay, R. (2012), "Analytical Assessment of Stability of Unbraced Column in Two Panel Concentrically Braced Frames," *3rd International Structural Specialty Conference,* Edmonton, Alberta, Canada, Paper No. 1218.

Imanpour, A. and Tremblay, R. (2014), "Seismic Design of Steel Multi-Tiered Braced Frames: Application of Incremental Static Analysis for Design of Steel Multi-Tiered Braced Frames," *EUROSTEEL 2014,* September 10-14, Napoli, Italy.

Imanpour, A. and Tremblay, R. (2016), "Analysis Methods for the Design of Special Concentrically Braced Frames with Three or More Tiers for In-Plane Seismic Demand," *Journal of Structural Engineering*, Vol. 143, No. 4, 04016213.

Imanpour, A., Tremblay, R., Davaran, A., Stoakes, C., and Fahnestock, L.A. (2016a), "Seismic Performance Assessment of Multitiered Steel Concentrically Braced Frames Designed in Accordance with the 2010 AISC Seismic Provisions," *Journal of Structural Engineering,* Vol. 142, No. 12, 4016135.

Imanpour, A., Tremblay, R., Fahnestock, L.A., and Stoakes, C. (2016b), "Analysis and Design of Two-Tiered Steel Braced Frames under In-Plane Seismic Demand," *Journal of Structural Engineering*, Vol. 142, No. 2.

Imanpour, A., Tremblay, R., Leclerc, M., and Siguier, R. (2018), "Development of a Hybrid Simulation Computational Model for Steel Braced Frames," *Key Engineering Materials,* Vol. 763, pp. 609–618, Trans Tech Publications.

Kazemzadeh Azad, S., Topkaya, C., and Bybordiani, M. (2018), "Dynamic Buckling of Braces in Concentrically Braced Frames," *Earthquake Engineering Structural Dynamics*, Vol. 47, pp. 613–633. DOI: https://doi.org/10.1002/eqe.2982.

Nakashima, M. and Wakabayashi, M. (1992), "Analysis and Design of Steel Braces and Braced Frames in Building Structures," *Stability and Ductility of Steel Structures under Cyclic Loading*, Y. Fukumoto and G.C. Lee, eds., CRC Press, Boca Raton, Fla., pp. 309–321.

Sabelli, R. and Hohbach, D. (1999), "Design of Cross-Braced Frames for Predictable Buckling Behavior," *Journal of Structural Engineering*, Vol. 125, No. 2, pp. 163–168.

Schmidt, B.J. and Bartlett, F.M. (2002), "Review of Resistance Factor for Steel: Data Collection," *Canadian Journal of Civil Engineering*, Vol. 29, pp. 109–118.

S-Frame Software [Computer Software] (2017), Structural analysis software.

Stoakes, C.D. and Fahnestock, L. A. (2014), "Three-Dimensional Finite Element Simulation of the Seismic Behavior of Multitier Concentrically Braced Frames," *Procedings of Structures Congress 2014*, pp. 2,675–2,686.

Stoakes, C.D. and Fahnestock, L. A. (2016), "Strong-Axis Stability of Wide Flange Steel Columns in the Presence of Weak-Axis Flexure," *Journal of Structural Engineering*, ASCE, January, DOI: 10.1061/(ASCE)ST.1943-541X.0001448.

Suzuki, Y. and Lignos, D.G. (2015), "Large Scale Collapse Experiments of Wide Flange Steel Beam Columns," *Proceedings of the 8th International Conference on Behavior of Steel Structures in Seismic Areas (STESSA)*, Shanghai, China, July 1–3.

Tremblay, R., Archambault, M.-H., and Filiatrault, A. (2003), "Seismic Response of Concentrically Braced Steel Frames Made with Rectangular Hollow Bracing Members," *Journal of Structural Engineering*, Vol. 129, No. 12, pp. 1,626–1,636.

Wakabayashi, M., Matsui, C., Minami, K., and Mitani, I. (1974), "Inelastic Behavior of Full-Scale Steel Frames With and Without Bracings," *Bulletin of the Disaster Prevention Research Institute,* Kyoto University, Vol. 24, No. 216, pp. 1–23.